

Quantifying quark mass effects at the LHC: a study of $pp \rightarrow b\bar{b}b\bar{b} + X$ at next-to-leading order

G. Bevilacqua, M. Czakon, M. Krämer, M. Kubocz and M. Worek

*Institute for Theoretical Particle Physics and Cosmology,
RWTH Aachen University, D-52056 Aachen, Germany*

E-mail: bevilacqua@physik.rwth-aachen.de,
mczakon@physik.rwth-aachen.de, mkraemer@physik.rwth-aachen.de,
kubocz@physik.rwth-aachen.de, worek@physik.rwth-aachen.de

ABSTRACT: The production of four bottom quarks is an important benchmark channel for Higgs analyses and searches for new physics at the LHC. We report on the calculation of the next-to-leading order QCD corrections to the process $pp \rightarrow b\bar{b}b\bar{b} + X$ with the HELAC-NLO automated framework, and present results for inclusive cross sections and differential distributions. We discuss the impact of the higher-order corrections and, in particular, the effect of the bottom quark mass. In addition, we provide an estimate of the theoretical uncertainty from the variation of the renormalisation and factorisation scales and the parton distribution functions. The results are obtained with a new subtraction formalism for real radiation at next-to-leading order, implemented in the HELAC-DIPOLES package.

KEYWORDS: QCD Phenomenology, NLO Computations

Contents

1	Introduction	1
2	Theoretical framework	2
3	Numerical results for the LHC	3
3.1	Massless bottom quarks within the five-flavour scheme	3
3.2	Massive bottom quarks within the four-flavour scheme	6
3.3	Comparison with results presented in the literature	8
4	Summary	10

1 Introduction

The production of four bottom quarks, $pp \rightarrow b\bar{b}b\bar{b} + X$, is an important background to various Higgs analyses and new physics searches at the LHC, including for example Higgs-boson pair production in two-Higgs doublet models at large $\tan\beta$ [1], or so-called hidden valley scenarios where additional gauge bosons can decay into bottom quarks [2, 3]. Accurate theoretical predictions for the Standard Model production of multiple bottom quarks are thus mandatory to exploit the potential of the LHC for new physics searches. Furthermore, the calculation of the next-to-leading order (NLO) QCD corrections to $pp \rightarrow b\bar{b}b\bar{b} + X$ provides a substantial technical challenge and requires the development of efficient techniques, with a high degree of automation. We have performed a NLO calculation of $b\bar{b}b\bar{b}$ production at the LHC with the HELAC-NLO system [4]. In particular, we present results based on a new subtraction formalism [5, 6] for treating real radiation corrections, as implemented in the HELAC-DIPOLES package [7]. Two calculation schemes have been employed, the so-called four-flavour scheme (4FS) with only gluons and light-flavour quarks in the proton, where massive bottom quarks are produced from gluon splitting at short distances, and the five-flavour-scheme (5FS) [8] with massless bottom quarks as partons in the proton. At all orders in perturbation theory, the four- and five-flavour schemes are identical, but the way of ordering the perturbative expansion is different, and at any finite order the results do not match. Comparing the predictions of the two schemes at NLO thus provides a way to assess the theoretical uncertainty from unknown higher-order corrections, and to study the effect of the bottom mass on the inclusive cross section and on differential distributions. First NLO results for $pp \rightarrow b\bar{b}b\bar{b} + X$ in the 5FS have been presented in ref. [9]. We not only provide an independent calculation of this challenging process with a different set of methods and tools, but also a systematic study of the bottom quark mass effects by comparing the 5FS and 4FS results. We note that NLO results for the production of four

top quarks in hadron collisions have been discussed in ref. [10]. In addition, NLO calculations for processes of similar complexity have recently been presented in the literature, including NLO QCD corrections to $t\bar{t}$ production in association with two jets [11–16], the production of a single gauge boson plus jets [17–20], double gauge boson production with two jets [21–25] and multi-jet production [26–28].

The paper is organised as follows. In section 2 we briefly summarise the set-up of the calculation. Numerical results for inclusive cross sections and differential distributions for $b\bar{b}b\bar{b}$ production at the LHC are presented in section 3. We summarise in section 4.

2 Theoretical framework

The calculation of the process $pp \rightarrow b\bar{b}b\bar{b} + X$ at NLO QCD comprises the parton processes $gg \rightarrow b\bar{b}b\bar{b}$ and $q\bar{q} \rightarrow b\bar{b}b\bar{b}$ at tree-level and including one-loop corrections, as well as the tree-level parton processes $gg \rightarrow b\bar{b}b\bar{b} + g$, $q\bar{q} \rightarrow b\bar{b}b\bar{b} + g$, $gq \rightarrow b\bar{b}b\bar{b} + q$ and $g\bar{q} \rightarrow b\bar{b}b\bar{b} + \bar{q}$. In the four-flavour scheme $q \in \{u, d, c, s\}$, and the bottom quark is treated massive. The bottom mass effects are in general suppressed by powers of m_b/μ , where μ is the hard scale of the process, e.g. the transverse momentum of a bottom-jet. Potentially large logarithmic corrections $\propto \ln(m_b/\mu)$ could arise from nearly collinear splitting of initial-state gluons into bottom quarks, $g \rightarrow b\bar{b}$, where the bottom mass acts as a regulator of the collinear singularity. This class of $\ln(m_b/\mu)$ -terms can be summed to all orders in perturbation theory by introducing bottom parton densities in the five-flavour scheme. The 5FS is based on the approximation that the bottom quarks from the gluon splitting are produced at small transverse momentum. However, in our calculation we require that all four bottom quarks can be experimentally detected, and we thus impose a lower cut on the bottom transverse momentum, $p_{T,b} \geq p_{T,b}^{\min}$. As a result, up to NLO accuracy the potentially large logarithms in the process $pp \rightarrow b\bar{b}b\bar{b} + X$ are replaced by $\ln(m_b/\mu) \rightarrow \ln(p_{T,b}^{\min}/\mu)$, with $m_b \ll p_{T,b}^{\min} \lesssim \mu$, and are thus much less significant numerically. Therefore, for the process at hand, the differences between the 4FS and 5FS calculations with massive and massless bottom quarks, respectively, should be moderate, but may not be completely negligible.

Our calculation is performed with the automated HELAC-NLO framework [4], which includes HELAC-1LOOP [29] for the evaluation of the numerators of the loop integrals and the rational terms, CUTTOOLS [30], which implements the OPP reduction method [31–34] to compute one-loop amplitudes, and ONELOOP [35] for the evaluation of the scalar integrals. The singularities for soft and collinear parton emission are treated using subtraction schemes as implemented in HELAC-DIPOLES [7], see the discussion below. The phase space integration is performed with the help of the Monte Carlo generators HELAC-PHEGAS [36–38] and KALEU [39], including PARNI [40] for the importance sampling.

The HELAC-DIPOLES package has been based on the standard Catani-Seymour dipole subtraction formalism [41, 42]. We have now extended HELAC-DIPOLES by implementing a new subtraction scheme [5, 6] using the momentum mapping and the splitting functions derived in the context of an improved parton shower formulation by Nagy and Soper [43]. Compared to standard dipole subtraction, the new scheme features a significantly smaller number of subtraction terms and facilitates the matching of NLO calculations with parton

showers including quantum interference. The results presented here constitute the first application of the Nagy-Soper subtraction scheme for a $2 \rightarrow 4$ scattering process with massive and massless fermions. A detailed description of the implementation of the new scheme, and a comparative study of the numerical efficiency and the speed will be presented elsewhere.

3 Numerical results for the LHC

In this section we present cross-section predictions for the process $pp \rightarrow b\bar{b}b\bar{b} + X$ at the LHC at the centre-of-mass energy of $\sqrt{s} = 14$ TeV. We discuss the impact of the NLO-QCD corrections, and study the dependence of the results on the bottom quark mass. We show results obtained with the standard dipole subtraction scheme for real radiation, and with the new subtraction formalism [5, 6] as implemented in HELAC-DIPOLES.

Let us first specify the input parameters and the acceptance cuts we impose. The top quark mass, which appears in the loop corrections, is set to $m_t = 173.5$ GeV [44]. We combine collinear final-state partons with pseudo-rapidity $|\eta| < 5$ into jets according to the anti- k_T algorithm [45] with separation $R = 0.4$. The bottom-jets have to pass the transverse momentum and rapidity cuts $p_{T,b} > 30$ GeV and $|y_b| < 2.5$, respectively. The renormalisation and factorisation scales are set to the scalar sum of the bottom-jet transverse masses, $\mu_R = \mu_F = \mu_0 = H_T$, with $H_T = m_{T,b} + m_{T,\bar{b}} + m_{T,b} + m_{T,\bar{b}}$ and the transverse mass $m_{T,b} = \sqrt{m_b^2 + p_{T,b}^2}$. For the five-flavour scheme calculation with massless bottom quarks the transverse mass equals the transverse momentum, $m_{T,b} = p_{T,b}$. Note that the implementation of a dynamical scale requires a certain amount of care, as the subtraction terms for real radiation have to be evaluated with a different kinematical configuration specified by the momentum mapping of the subtraction scheme. Comparing our results as obtained with the Catani-Seymour subtraction and the Nagy-Soper scheme, which is based on a different momentum mapping, provides an important and highly non-trivial internal check of our calculation.

3.1 Massless bottom quarks within the five-flavour scheme

Results are presented for the NLO CT10 [46] and MSTW2008 [47] parton distribution functions (pdfs) with five active flavours and the corresponding two-loop α_s . To study the impact of the higher-order corrections, we also show leading-order results obtained using the CT09MC1 [48] and MSTW2008 LO pdf sets and one-loop running for α_s .

We first discuss the impact of the bottom-quark induced processes, $b\bar{b} \rightarrow b\bar{b}b\bar{b}$, on the hadronic cross section at leading-order. The difference between the $q\bar{q}$ initiated processes, $q\bar{q} \rightarrow b\bar{b}b\bar{b}$, with and without bottom-quarks is at the level of 2.5%. Moreover, at the central scale, $\mu = H_T$, the hadronic cross section is completely dominated by gluon-fusion, with only about 1% contribution of all quark-antiquark annihilation processes. The bottom-induced contributions are thus negligible, and we decided to neglect bottom initial states in the computation of the cross section both at LO and NLO. Note that the suppression of the bottom-induced processes, which include for example potentially large forward scattering of bottom-quarks through t -channel gluon exchange, depends crucially on the transverse momentum cuts we impose on the bottom-jets.

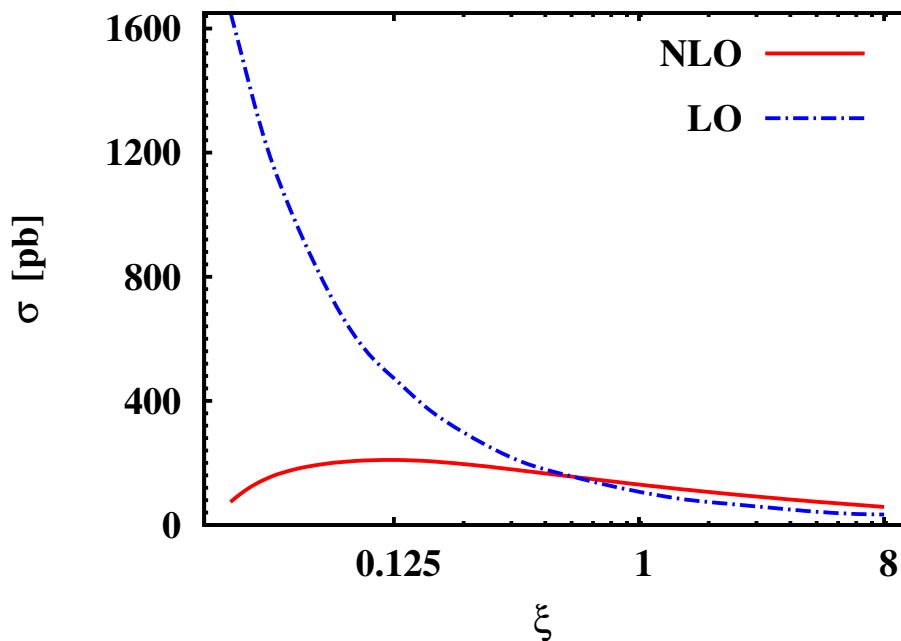


Figure 1. Scale dependence of the 5FS LO and NLO cross sections for $pp \rightarrow b\bar{b}b\bar{b} + X$ at the LHC ($\sqrt{s} = 14$ TeV). The renormalisation and factorisation scales are set to a common value $\mu_R = \mu_F = \xi \mu_0$ where $\mu_0 = H_T$. The CT09MC1 and CT10 pdf sets have been used for the LO and NLO cross sections, respectively. Kinematical cuts are listed in section 3.

$pp \rightarrow b\bar{b}b\bar{b} + X$	σ_{LO} [pb]	σ_{NLO} [pb]	$K = \sigma_{\text{NLO}}/\sigma_{\text{LO}}$
CT09MC1/CT10	$106.9^{+61.5 (57\%)}_{-36.4 (34\%)}$	$123.6^{+35.6 (29\%)}_{-26.6 (22\%)}$	1.15
MSTW2008LO/NLO	$99.9^{+58.7 (59\%)}_{-34.9 (35\%)}$	$136.7^{+38.8(28\%)}_{-30.9 (23\%)}$	1.37

Table 1. 5FS LO and NLO cross sections for $pp \rightarrow b\bar{b}b\bar{b} + X$ at the LHC ($\sqrt{s} = 14$ TeV). The renormalisation and factorisation scales have been set to the central value $\mu_0 = H_T$, and the uncertainty is estimated by varying both scales simultaneously by a factor two about the central scale. Results are shown for the CT09MC1/CT10 and MSTW2008LO/NLO pdf sets. Kinematical cuts are listed in section 3.

Let us first present our results for the inclusive cross section $pp \rightarrow b\bar{b}b\bar{b} + X$ at the LHC ($\sqrt{s} = 14$ TeV), including the transverse momentum and rapidity cuts specified at the beginning of the section. The NLO QCD corrections strongly reduce the scale dependence, as demonstrated in figure 1. The central cross section predictions are collected in table 1. Varying the renormalisation and factorisation scales simultaneously about the central scale by a factor of two, we find a residual scale uncertainty of approximately 30% at NLO, a reduction by about a factor of two compared to LO. The size of the K -factor, $K = \sigma_{\text{NLO}}/\sigma_{\text{LO}}$, strongly depends on the pdf set, with $K = 1.15$ for CT10 and $K = 1.37$ for MSTW2008. We emphasise, however, that the K -factor is an unphysical quantity and strongly sensitive to the choice of scale through the large LO scale dependence.

$pp \rightarrow b\bar{b}b\bar{b} + X$	$\sigma_{\text{NLO}}^{\text{CS}(\alpha_{\text{max}}=1)}$ [pb]	$\sigma_{\text{NLO}}^{\text{CS}(\alpha_{\text{max}}=0.01)}$ [pb]	$\sigma_{\text{NLO}}^{\text{NS}}$ [pb]
CT10	123.6 ± 0.4	124.9 ± 0.9	124.8 ± 0.3
MSTW2008NLO	136.7 ± 0.3	136.1 ± 0.5	137.6 ± 0.5

Table 2. 5FS NLO cross sections for $pp \rightarrow b\bar{b}b\bar{b} + X$ at the LHC ($\sqrt{s} = 14$ TeV). Results are shown for two different subtraction schemes, the Catani-Seymour (CS) dipole subtraction, without ($\alpha_{\text{max}} = 1$) and with ($\alpha_{\text{max}} = 0.01$) a restriction on the phase space of the subtraction, and the new Nagy-Soper (NS) scheme, including the numerical error from the Monte Carlo integration. The renormalisation and factorisation scales have been set to the central value $\mu_0 = H_T$, and the CT10 and MSTW2008NLO pdf sets have been employed. Kinematical cuts are listed in section 3.

We observe a difference of about -7% and $+11\%$ between the CT10 and MSTW2008 pdf parametrisations at LO and NLO, respectively. The pdf uncertainty as estimated from the MSTW2008 error pdf sets [47] amounts to $+7.3\%$ and -1.5% at 68% C.L., and is significantly smaller than the scale uncertainty. A more systematic discussion of pdf and α_s uncertainties will thus be referred to a forthcoming publication.

An important input for the experimental analyses and the interpretation of the experimental data are accurate predictions of differential distributions. Our calculation is set up as a parton-level Monte Carlo program and thus allows us to predict any infrared-safe observable at NLO. Figure 2 shows LO and NLO predictions for the invariant mass of the $b\bar{b}b\bar{b}$ system (upper left panel), the total transverse energy H_T (upper right panel), the transverse momentum of the hardest bottom jet (lower left panel) and the transverse momentum of the second hardest bottom jet (lower right panel). We also show the theoretical uncertainty through scale variation and the K -factor as a function of the kinematic variable. It is evident from figure 2 that the NLO corrections significantly reduce the theoretical uncertainty of the differential distributions, and that the size of the higher-order effects depends on the kinematics. For an accurate description of exclusive observables and differential distributions it is thus not sufficient to rescale a LO prediction with an inclusive K -factor.

As discussed in section 2 we have performed the calculation with two different subtraction schemes, the standard Catani-Seymour (CS) dipole subtraction, and a new scheme based on the splitting functions and momentum mapping of an improved parton shower by Nagy and Soper (NS). The comparison between the two schemes for the inclusive 5FS cross section is presented in table 2. For the Catani-Seymour scheme we show results without ($\alpha_{\text{max}} = 1$) and with ($\alpha_{\text{max}} = 0.01$) a restriction on the phase space of the subtraction as proposed in ref. [49–51]. As evident from table 2, the cross sections obtained using the Catani-Seymour (CS) and Nagy-Soper (NS) subtraction schemes agree within the numerical uncertainty of the Monte Carlo integration. This result not only provides a validation of our implementation of the new subtraction scheme into HELAC-DIPOLES, but also provides a non-trivial internal cross check of the calculation.

We have also compared the results obtained in the CS and NS subtraction schemes for various differential distributions. Some examples are collected in figure 3. We observe full agreement between the predictions calculated with the two schemes.

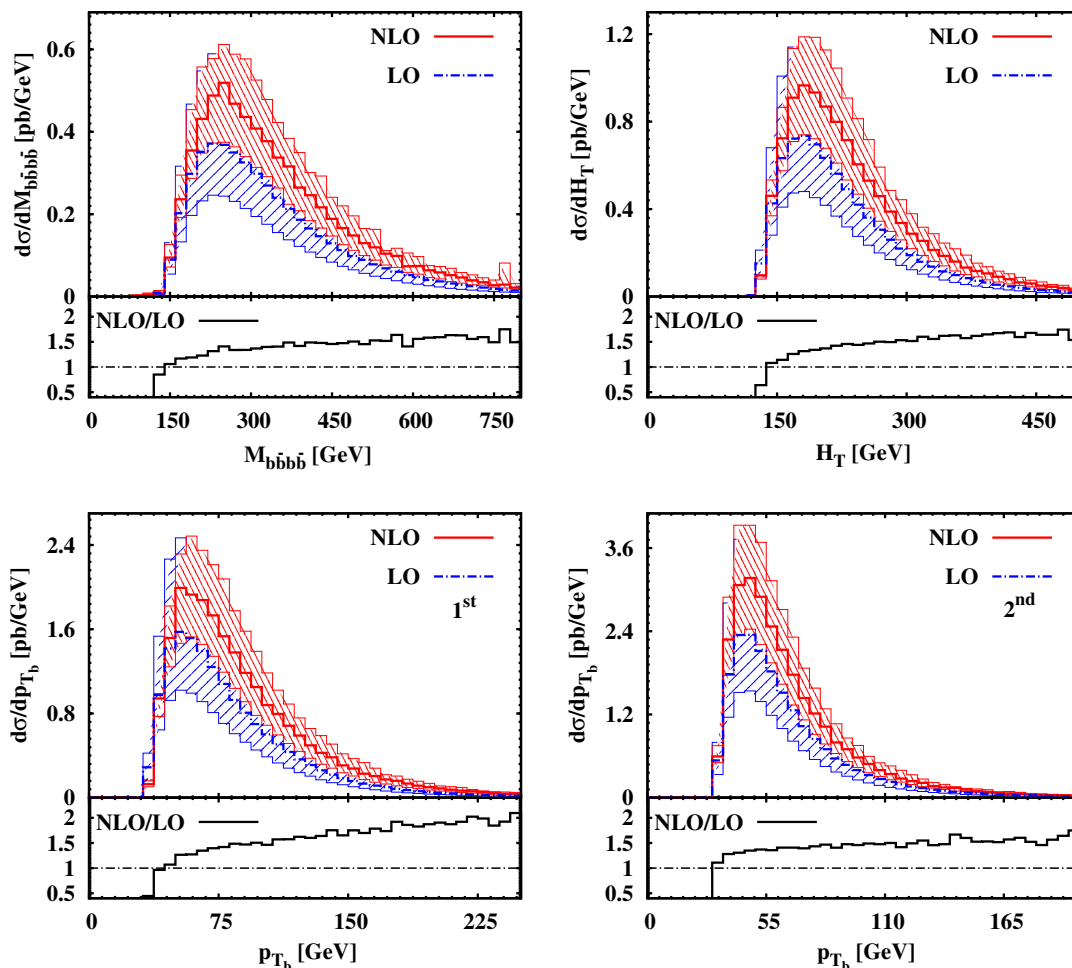


Figure 2. Differential cross section for $pp \rightarrow b\bar{b}b\bar{b} + X$ at the LHC ($\sqrt{s} = 14$ TeV) in the 5FS as a function of the invariant mass of the $b\bar{b}b\bar{b}$ system (upper left panel), the total transverse energy of the system (upper right panel), the transverse momentum of the hardest bottom jet (lower left panel) and the transverse momentum of the second hardest bottom jet (lower right panel). The dash-dotted (blue) curve corresponds to the LO and the solid (red) curve to the NLO result. The scale choice is $\mu_R = \mu_F = \mu_0 = H_T$. The hashed area represents the scale uncertainty, and the lower panels display the differential K factor. The cross sections are evaluated with the MSTW2008 pdf sets. Kinematical cuts are listed in section 3.

3.2 Massive bottom quarks within the four-flavour scheme

Within the four-flavour scheme bottom quarks are treated massive and are not included in the parton distribution functions of the proton. We define the bottom quark mass in the on-shell scheme and use $m_b = 4.75$ GeV, consistent with the choice made in the MSTW2008 four-flavour pdf. The central cross section prediction in LO and NLO for $\mu = H_T$ using the 4FS MSTW2008 [52] pdf are shown in table 3. Comparing with the 5FS results presented in table 1, we observe that the bottom mass effects decrease the cross section prediction by 18% at LO and 16% at NLO. The residual scale dependence at NLO is approximately 30%, similar to the 5FS calculation.

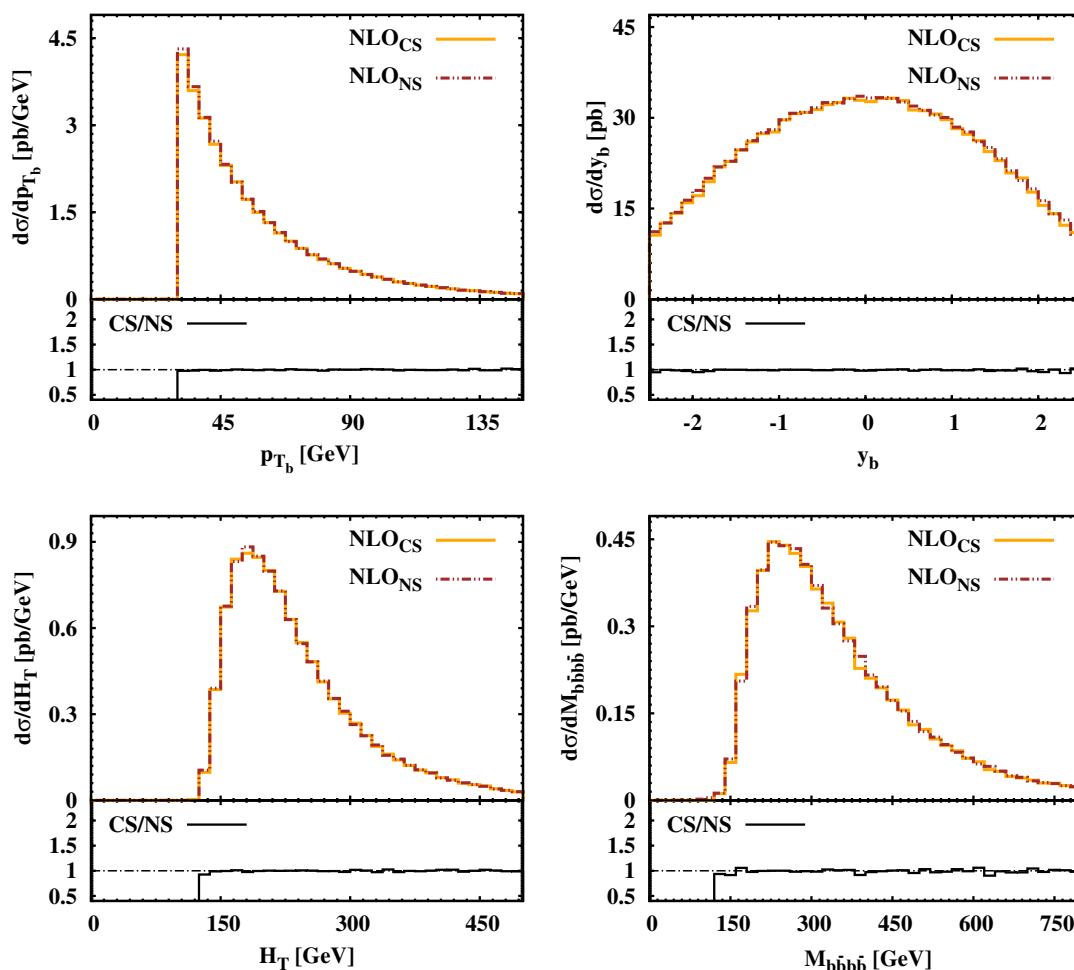


Figure 3. Differential cross section for $pp \rightarrow b\bar{b}b\bar{b} + X$ at the LHC ($\sqrt{s} = 14$ TeV) in the 5FS as a function of the average transverse momentum of the bottom jets (upper left panel), the average rapidity of the bottom jets (upper right panel), the total transverse energy (lower left panel) and the $b\bar{b}b\bar{b}$ invariant mass (lower right panel). The dash-dotted (brown) curve corresponds to the Catani-Seymour (CS) and the solid (orange) curve to the Nagy-Soper (NS) subtraction schemes, respectively. The lower panels show the ratio of the results within the two schemes. The scale choice is $\mu_R = \mu_F = \mu_0 = H_T$, the cross sections are evaluated with the CT10 pdf set. Kinematical cuts are listed in section 3.

$pp \rightarrow b\bar{b}b\bar{b} + X$	σ_{LO} [pb]	σ_{NLO} [pb]	$K = \sigma_{\text{NLO}}/\sigma_{\text{LO}}$
MSTW2008LO/NLO (4FS)	$84.5^{+49.7(59\%)}_{-29.6(35\%)}$	$118.3^{+33.3(28\%)}_{-29.0(24\%)}$	1.40

Table 3. 4FS LO and NLO cross sections for $pp \rightarrow b\bar{b}b\bar{b} + X$ at the LHC ($\sqrt{s} = 14$ TeV). The renormalisation and factorisation scales have been set to the central value $\mu_0 = H_T$, and the uncertainty is estimated by varying both scales simultaneously by a factor two about the central scale. Results are shown for the 4FS MSTW2008LO/NLO pdf sets. Kinematical cuts are listed in section 3.

$pp \rightarrow b\bar{b}b\bar{b} + X$	$\sigma_{\text{NLO}}^{\text{CS}(\alpha_{\text{max}}=1)}$ [pb]	$\sigma_{\text{NLO}}^{\text{CS}(\alpha_{\text{max}}=0.01)}$ [pb]	$\sigma_{\text{NLO}}^{\text{NS}}$ [pb]
MSTW2008NLO (4FS)	118.3 ± 0.5	118.2 ± 0.7	118.0 ± 0.5

Table 4. 4FS NLO cross sections for $pp \rightarrow b\bar{b}b\bar{b} + X$ at the LHC ($\sqrt{s} = 14$ TeV). Results are shown for two different subtraction schemes, the Catani-Seymour (CS) dipole subtraction, without ($\alpha_{\text{max}} = 1$) and with ($\alpha_{\text{max}} = 0.01$) restriction on the phase space of the subtraction, and the new Nagy-Soper (NS) scheme, including the numerical error from the Monte Carlo integration. The renormalisation and factorisation scales have been set to the central value $\mu_0 = H_T$, and the MSTW2008NLO 4FS pdf set has been employed. Kinematical cuts are listed in section 3.

The difference between the massless 5FS and the massive 4FS calculations has two origins. First, there are genuine bottom mass effects, the size of which depends sensitively on the transverse momentum cut. For $p_{T,b}^{\text{min}} = 30$ GeV we find a 10% difference between the 5FS and 4FS from non-singular bottom-mass dependent terms. This difference decreases to about 1% for $p_{T,b}^{\text{min}} = 100$ GeV. Second, the two calculations involve different pdf sets and different corresponding α_s . While a 4FS pdf has, in general, a larger gluon flux than a 5FS pdf, as there is no $g \rightarrow b\bar{b}$ splitting, the corresponding four-flavour α_s is smaller than for five active flavours. For $pp \rightarrow b\bar{b}b\bar{b} + X$ the difference in α_s is prevailing and results in a further reduction of the 4FS cross section prediction by about 5%. This latter difference should be viewed as a scheme dependence rather than a bottom mass effect.

In figure 4 we present the differential distribution in the transverse momentum of the hardest bottom jet, as calculated in the 5FS with massless bottom quarks and in the 4FS with $m_b = 4.75$ GeV. We show the absolute prediction at LO and NLO, and the predictions normalised to the corresponding inclusive cross section. The latter plots reveal that the difference in the shape of the distributions in the 5FS and the 4FS is very small. We find similar results for other differential distributions. Let us mention here that at NLO substantial fluctuations are visible as compared to LO. However, these fluctuations are caused by the limited statistics of the NLO Monte Carlo integration.

Let us finally present the comparison of the massive bottom quark results as obtained with the Catani-Seymour and Nagy-Soper subtraction schemes, see table 4. We observe full agreement between the two calculations within the numerical error of the Monte Carlo integration, and thereby validate our implementation of the NS subtraction scheme also for the case of massive fermions.

3.3 Comparison with results presented in the literature

A detailed comparison of our results with ref. [9] has been performed. We find agreement for the virtual amplitude at one specific phase space point, but cannot reproduce the published results for the integrated hadronic LO and NLO cross sections with the setup as described in ref. [9]. When the CTEQ6.5 pdf set [53] is used rather than CTEQ6M [54] as specified in [9], and the factorization and renormalization scales are set to the common value

$$\mu_0 = \frac{1}{4} \sqrt{\sum_i p_{T,i}^2}, \tag{3.1}$$

the LO result published in [9] can be reproduced as shown in table 5.

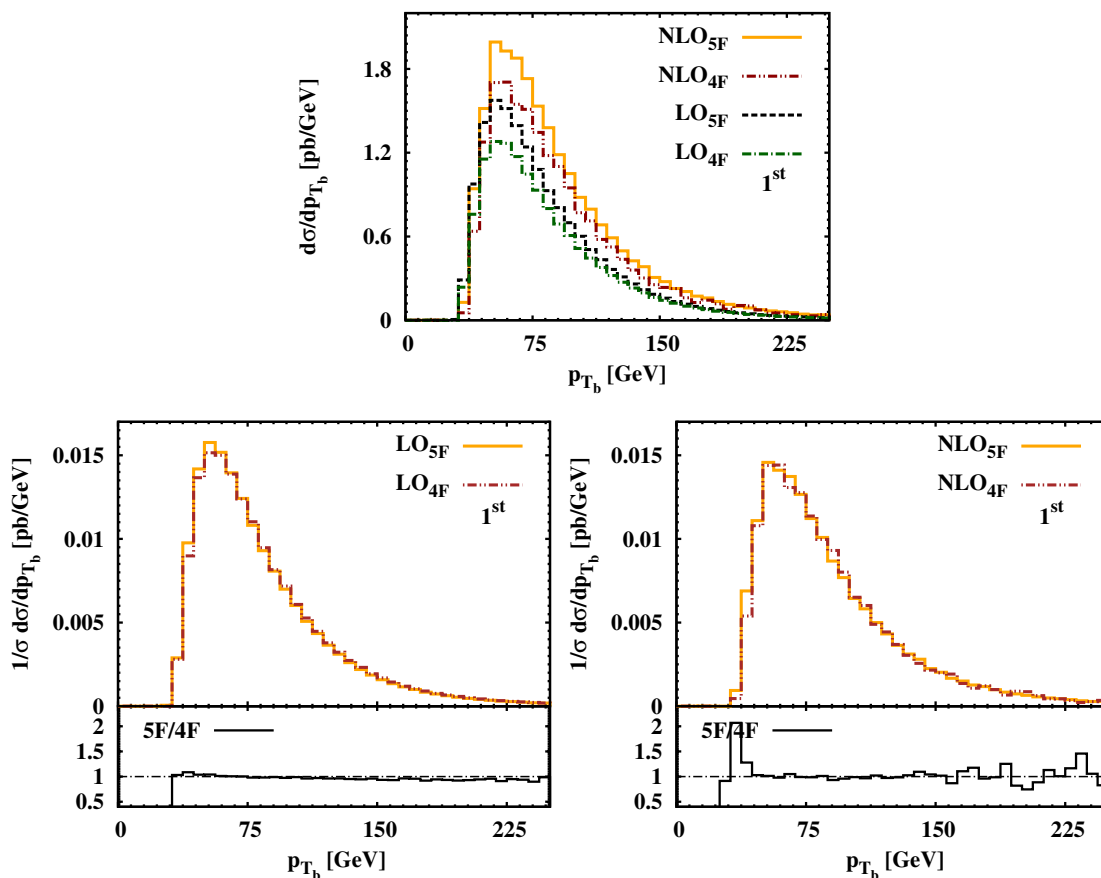


Figure 4. Differential cross section for $pp \rightarrow b\bar{b}b\bar{b} + X$ at the LHC ($\sqrt{s} = 14$ TeV) in the 4FS and 5FS as a function of the transverse momentum of the hardest bottom jet. Also shown are the normalised distributions at LO (lower left panel) and at NLO (lower right panel). The lower panels show the ratio of the results within the two schemes. The scale choice is $\mu_R = \mu_F = \mu_0 = H_T$, the cross sections are evaluated with the 5FS and 4FS MSTW2008 pdf sets, respectively. Kinematical cuts are listed in section 3.

$\sigma_{\text{LO}}^{[9]}$ [pb]	σ_{LO} [pb]
94.88 ± 0.14	94.74 ± 0.20

Table 5. LO cross section for $pp \rightarrow b\bar{b}b\bar{b} + X$ at the LHC ($\sqrt{s} = 14$ TeV) in comparison with the result of ref. [9]. Results are shown including the numerical error from the Monte Carlo integration. The scale choice is $\mu_R = \mu_F = \mu_0$, with μ_0 as defined in eq. (3.1), and the cross sections are evaluated with the CTEQ6.5 pdf set. Kinematical cuts are taken from ref. [9].

After comprehensive numerical checks and the communication with the authors of ref. [9] it turned out that the NLO numbers published in [9] are based on a scale setting that mixes partons and jets and that is not consistent with what is specified in ref. [9]. Adopting $\mu_R = \mu_F = \mu_0$, with μ_0 defined in eq. (3.1), and summing over the transverse momenta of all jets, we obtain the NLO numbers presented in table 6. Note that at NLO

$\sigma_{\text{NLO}}^{[9]}$ [pb]	$\sigma_{\text{NLO}}^{[9], \text{corr.}}$ [pb]	$\sigma_{\text{NLO}}^{\text{CS}(\alpha_{\text{max}}=0.01)}$ [pb]	$\sigma_{\text{NLO}}^{\text{CS}(\alpha_{\text{max}}=1)}$ [pb]	$\sigma_{\text{NLO}}^{\text{NS}}$ [pb]
140.48 ± 0.64	143.75 ± 0.67	143.70 ± 0.44	144.35 ± 0.53	144.73 ± 0.62

Table 6. NLO cross sections for $pp \rightarrow b\bar{b}b\bar{b} + X$ at the LHC ($\sqrt{s} = 14$ TeV) in comparison with published results of ref. [9], $\sigma_{\text{NLO}}^{[9]}$, and a corrected result based on the calculation of ref. [9], $\sigma_{\text{NLO}}^{[9], \text{corr.}}$ (private communication). Our results are shown for two different subtraction schemes, the Catani-Seymour (CS) dipole subtraction, without ($\alpha_{\text{max}} = 1$) and with ($\alpha_{\text{max}} = 0.01$) restriction on the phase space of the subtraction, and the new Nagy-Soper (NS) scheme, including the numerical error from the Monte Carlo integration. The scale choice is $\mu_R = \mu_F = \mu_0$, with μ_0 as defined in eq. (3.1), and the cross sections are evaluated with the CTEQ6.5 pdf set. Kinematical cuts are taken from ref. [9].

the final state can consist of four or five jets, as determined by the jet algorithm. Our results are compared to the NLO number as published in ref. [9], $\sigma_{\text{NLO}}^{[9]}$, and to a corrected number obtained by means of private communication from the authors of ref. [9], $\sigma_{\text{NLO}}^{[9], \text{corr.}}$. The corrected result agrees with our calculation.

Also note that in ref. [9] an NLO pdf set has been used both for the LO and NLO result. Although this may be justified to study the impact of higher-order corrections to the partonic cross section, it can be misleading when establishing the genuine effect of higher-order corrections, the adequacy of the scale choice or the size/shape of integrated/differential K -factors used in experimental analyses when comparing Monte Carlo simulations to the LHC data.

4 Summary

The production of four bottoms quarks, $pp \rightarrow b\bar{b}b\bar{b} + X$, provides an important background for new physics searches at the LHC. We have performed a calculation of the NLO QCD corrections to this process with the HELAC-NLO framework, employing a new subtraction scheme for treating real radiation corrections at NLO implemented in HELAC-DIPOLES. Results have been presented for inclusive and differential cross-sections for $pp \rightarrow b\bar{b}b\bar{b} + X$ at the LHC at the centre-of-mass energy of $\sqrt{s} = 14$ TeV. We find that the higher-order corrections significantly reduce the scale dependence, with a residual theoretical uncertainty of about 30% at NLO. The impact of the bottom quark mass is moderate for the cross section normalisation and negligible for the shape of distributions. The fully differential NLO cross section calculation for the process $pp \rightarrow b\bar{b}b\bar{b} + X$ presented in this paper provides an important input for the experimental analyses and the interpretation of new physics searches at the LHC.

Acknowledgments

The calculations have been performed on the Grid Cluster of the Bergische Universität Wuppertal, financed by the Helmholtz-Alliance “Physics at the Terascale” and the BMBF.

We acknowledge the correspondence with Nicolas Greiner on the results of ref. [9] and discussions with Zoltan Nagy. This research was supported in part by the German Research Foundation (DFG) via the Sonderforschungsbereich/Transregio SFB/TR-9 “Computational Particle Physics”. The work of M.C. was supported by the DFG Heisenberg program. M.W. acknowledges support by the DFG under Grant No. WO 1900/1-1 (“Signals and Backgrounds Beyond Leading Order. Phenomenological studies for the LHC”).

References

- [1] J. Dai, J. Gunion and R. Vega, *Detection of neutral MSSM Higgs bosons in four b final states at the Tevatron and the LHC: an update*, *Phys. Lett. B* **387** (1996) 801 [[hep-ph/9607379](#)] [[INSPIRE](#)].
- [2] M.J. Strassler and K.M. Zurek, *Echoes of a hidden valley at hadron colliders*, *Phys. Lett. B* **651** (2007) 374 [[hep-ph/0604261](#)] [[INSPIRE](#)].
- [3] M. Gouzevitch et al., *Scale-invariant resonance tagging in multijet events and new physics in Higgs pair production*, [arXiv:1303.6636](#) [[INSPIRE](#)].
- [4] G. Bevilacqua et al., *HELAC-NLO*, *Comput. Phys. Commun.* **184** (2013) 986 [[arXiv:1110.1499](#)] [[INSPIRE](#)].
- [5] C. Chung, M. Krämer and T. Robens, *An alternative subtraction scheme for next-to-leading order QCD calculations*, *JHEP* **06** (2011) 144 [[arXiv:1012.4948](#)] [[INSPIRE](#)].
- [6] C.-H. Chung and T. Robens, *Nagy-Soper subtraction scheme for multiparton final states*, *Phys. Rev. D* **87** (2013) 074032 [[arXiv:1209.1569](#)] [[INSPIRE](#)].
- [7] M. Czakon, C. Papadopoulos and M. Worek, *Polarizing the dipoles*, *JHEP* **08** (2009) 085 [[arXiv:0905.0883](#)] [[INSPIRE](#)].
- [8] R.M. Barnett, H.E. Haber and D.E. Soper, *Ultraheavy particle production from heavy partons at hadron colliders*, *Nucl. Phys. B* **306** (1988) 697 [[INSPIRE](#)].
- [9] N. Greiner, A. Guffanti, T. Reiter and J. Reuter, *NLO QCD corrections to the production of two bottom-antibottom pairs at the LHC*, *Phys. Rev. Lett.* **107** (2011) 102002 [[arXiv:1105.3624](#)] [[INSPIRE](#)].
- [10] G. Bevilacqua and M. Worek, *Constraining BSM physics at the LHC: four top final states with NLO accuracy in perturbative QCD*, *JHEP* **07** (2012) 111 [[arXiv:1206.3064](#)] [[INSPIRE](#)].
- [11] A. Bredenstein, A. Denner, S. Dittmaier and S. Pozzorini, *NLO QCD corrections to $pp \rightarrow t\bar{t}b\bar{b} + X$ at the LHC*, *Phys. Rev. Lett.* **103** (2009) 012002 [[arXiv:0905.0110](#)] [[INSPIRE](#)].
- [12] G. Bevilacqua, M. Czakon, C. Papadopoulos, R. Pittau and M. Worek, *Assault on the NLO wishlist: $pp \rightarrow t\bar{t}b\bar{b}$* , *JHEP* **09** (2009) 109 [[arXiv:0907.4723](#)] [[INSPIRE](#)].
- [13] A. Bredenstein, A. Denner, S. Dittmaier and S. Pozzorini, *NLO QCD corrections to top anti-top bottom anti-bottom production at the LHC: 2. full hadronic results*, *JHEP* **03** (2010) 021 [[arXiv:1001.4006](#)] [[INSPIRE](#)].
- [14] G. Bevilacqua, M. Czakon, C. Papadopoulos and M. Worek, *Dominant QCD backgrounds in Higgs boson analyses at the LHC: a study of $pp \rightarrow t\bar{t} + 2$ jets at next-to-leading order*, *Phys. Rev. Lett.* **104** (2010) 162002 [[arXiv:1002.4009](#)] [[INSPIRE](#)].

- [15] G. Bevilacqua, M. Czakon, C. Papadopoulos and M. Worek, *Hadronic top-quark pair production in association with two jets at next-to-leading order QCD*, *Phys. Rev. D* **84** (2011) 114017 [[arXiv:1108.2851](#)] [[INSPIRE](#)].
- [16] M. Worek, *On the next-to-leading order QCD K-factor for top anti-top bottom anti-bottom production at the Tevatron*, *JHEP* **02** (2012) 043 [[arXiv:1112.4325](#)] [[INSPIRE](#)].
- [17] C. Berger et al., *Precise predictions for $W + 3$ jet production at hadron colliders*, *Phys. Rev. Lett.* **102** (2009) 222001 [[arXiv:0902.2760](#)] [[INSPIRE](#)].
- [18] R.K. Ellis, K. Melnikov and G. Zanderighi, *$W + 3$ jet production at the Tevatron*, *Phys. Rev. D* **80** (2009) 094002 [[arXiv:0906.1445](#)] [[INSPIRE](#)].
- [19] C. Berger et al., *Precise predictions for $W + 4$ jet production at the Large Hadron Collider*, *Phys. Rev. Lett.* **106** (2011) 092001 [[arXiv:1009.2338](#)] [[INSPIRE](#)].
- [20] Z. Bern et al., *Next-to-leading order $W + 5$ -jet production at the LHC*, [arXiv:1304.1253](#) [[INSPIRE](#)].
- [21] A. Denner, S. Dittmaier, S. Kallweit and S. Pozzorini, *NLO QCD corrections to $WWbb$ production at hadron colliders*, *Phys. Rev. Lett.* **106** (2011) 052001 [[arXiv:1012.3975](#)] [[INSPIRE](#)].
- [22] G. Bevilacqua, M. Czakon, A. van Hameren, C.G. Papadopoulos and M. Worek, *Complete off-shell effects in top quark pair hadroproduction with leptonic decay at next-to-leading order*, *JHEP* **02** (2011) 083 [[arXiv:1012.4230](#)] [[INSPIRE](#)].
- [23] T. Melia, K. Melnikov, R. Rontsch and G. Zanderighi, *NLO QCD corrections for W^+W^- pair production in association with two jets at hadron colliders*, *Phys. Rev. D* **83** (2011) 114043 [[arXiv:1104.2327](#)] [[INSPIRE](#)].
- [24] N. Greiner et al., *NLO QCD corrections to the production of W^+W^- plus two jets at the LHC*, *Phys. Lett. B* **713** (2012) 277 [[arXiv:1202.6004](#)] [[INSPIRE](#)].
- [25] A. Denner, S. Dittmaier, S. Kallweit and S. Pozzorini, *NLO QCD corrections to off-shell top-antitop production with leptonic decays at hadron colliders*, *JHEP* **10** (2012) 110 [[arXiv:1207.5018](#)] [[INSPIRE](#)].
- [26] S. Becker, D. Goetz, C. Reuschle, C. Schwan and S. Weinzierl, *NLO results for five, six and seven jets in electron-positron annihilation*, *Phys. Rev. Lett.* **108** (2012) 032005 [[arXiv:1111.1733](#)] [[INSPIRE](#)].
- [27] Z. Bern et al., *Four-jet production at the Large Hadron Collider at next-to-leading order in QCD*, *Phys. Rev. Lett.* **109** (2012) 042001 [[arXiv:1112.3940](#)] [[INSPIRE](#)].
- [28] S. Badger, B. Biedermann, P. Uwer and V. Yundin, *NLO QCD corrections to multi-jet production at the LHC with a centre-of-mass energy of $\sqrt{s} = 8$ TeV*, *Phys. Lett. B* **718** (2013) 965 [[arXiv:1209.0098](#)] [[INSPIRE](#)].
- [29] A. van Hameren, C. Papadopoulos and R. Pittau, *Automated one-loop calculations: a proof of concept*, *JHEP* **09** (2009) 106 [[arXiv:0903.4665](#)] [[INSPIRE](#)].
- [30] G. Ossola, C.G. Papadopoulos and R. Pittau, *CutTools: a program implementing the OPP reduction method to compute one-loop amplitudes*, *JHEP* **03** (2008) 042 [[arXiv:0711.3596](#)] [[INSPIRE](#)].
- [31] G. Ossola, C.G. Papadopoulos and R. Pittau, *Reducing full one-loop amplitudes to scalar integrals at the integrand level*, *Nucl. Phys. B* **763** (2007) 147 [[hep-ph/0609007](#)] [[INSPIRE](#)].

- [32] G. Ossola, C.G. Papadopoulos and R. Pittau, *On the rational terms of the one-loop amplitudes*, *JHEP* **05** (2008) 004 [[arXiv:0802.1876](#)] [[INSPIRE](#)].
- [33] P. Mastrolia, G. Ossola, C. Papadopoulos and R. Pittau, *Optimizing the reduction of one-loop amplitudes*, *JHEP* **06** (2008) 030 [[arXiv:0803.3964](#)] [[INSPIRE](#)].
- [34] P. Draggiotis, M. Garzelli, C. Papadopoulos and R. Pittau, *Feynman rules for the rational part of the QCD 1-loop amplitudes*, *JHEP* **04** (2009) 072 [[arXiv:0903.0356](#)] [[INSPIRE](#)].
- [35] A. van Hameren, *OneLoop: for the evaluation of one-loop scalar functions*, *Comput. Phys. Commun.* **182** (2011) 2427 [[arXiv:1007.4716](#)] [[INSPIRE](#)].
- [36] A. Kanaki and C.G. Papadopoulos, *HELAC: a package to compute electroweak helicity amplitudes*, *Comput. Phys. Commun.* **132** (2000) 306 [[hep-ph/0002082](#)] [[INSPIRE](#)].
- [37] C.G. Papadopoulos, *PHEGAS: a phase space generator for automatic cross-section computation*, *Comput. Phys. Commun.* **137** (2001) 247 [[hep-ph/0007335](#)] [[INSPIRE](#)].
- [38] A. Cafarella, C.G. Papadopoulos and M. Worek, *Helac-Phegas: a generator for all parton level processes*, *Comput. Phys. Commun.* **180** (2009) 1941 [[arXiv:0710.2427](#)] [[INSPIRE](#)].
- [39] A. van Hameren, *Kaleu: a general-purpose parton-level phase space generator*, [arXiv:1003.4953](#) [[INSPIRE](#)].
- [40] A. van Hameren, *PARNI for importance sampling and density estimation*, *Acta Phys. Polon.* **B 40** (2009) 259 [[arXiv:0710.2448](#)] [[INSPIRE](#)].
- [41] S. Catani and M. Seymour, *A general algorithm for calculating jet cross-sections in NLO QCD*, *Nucl. Phys.* **B 485** (1997) 291 [*Erratum ibid.* **B 510** (1998) 503-504] [[hep-ph/9605323](#)] [[INSPIRE](#)].
- [42] S. Catani, S. Dittmaier, M.H. Seymour and Z. Trócsányi, *The Dipole formalism for next-to-leading order QCD calculations with massive partons*, *Nucl. Phys.* **B 627** (2002) 189 [[hep-ph/0201036](#)] [[INSPIRE](#)].
- [43] Z. Nagy and D.E. Soper, *Parton showers with quantum interference*, *JHEP* **09** (2007) 114 [[arXiv:0706.0017](#)] [[INSPIRE](#)].
- [44] PARTICLE DATA GROUP collaboration, J. Beringer et al., *Review of particle physics*, *Phys. Rev.* **D 86** (2012) 010001 [[INSPIRE](#)].
- [45] M. Cacciari, G.P. Salam and G. Soyez, *The anti- k_t jet clustering algorithm*, *JHEP* **04** (2008) 063 [[arXiv:0802.1189](#)] [[INSPIRE](#)].
- [46] H.-L. Lai et al., *New parton distributions for collider physics*, *Phys. Rev.* **D 82** (2010) 074024 [[arXiv:1007.2241](#)] [[INSPIRE](#)].
- [47] A. Martin, W. Stirling, R. Thorne and G. Watt, *Parton distributions for the LHC*, *Eur. Phys. J.* **C 63** (2009) 189 [[arXiv:0901.0002](#)] [[INSPIRE](#)].
- [48] H.-L. Lai et al., *Parton distributions for event generators*, *JHEP* **04** (2010) 035 [[arXiv:0910.4183](#)] [[INSPIRE](#)].
- [49] S. Frixione, Z. Kunszt and A. Signer, *Three jet cross-sections to next-to-leading order*, *Nucl. Phys.* **B 467** (1996) 399 [[hep-ph/9512328](#)] [[INSPIRE](#)].
- [50] Z. Nagy and Z. Trócsányi, *Next-to-leading order calculation of four jet observables in electron positron annihilation*, *Phys. Rev.* **D 59** (1999) 014020 [*Erratum ibid.* **D 62** (2000) 099902] [[hep-ph/9806317](#)] [[INSPIRE](#)].

- [51] Z. Nagy, *Next-to-leading order calculation of three jet observables in hadron hadron collision*, *Phys. Rev. D* **68** (2003) 094002 [[hep-ph/0307268](#)] [[INSPIRE](#)].
- [52] A. Martin, W. Stirling, R. Thorne and G. Watt, *Heavy-quark mass dependence in global PDF analyses and 3- and 4-flavour parton distributions*, *Eur. Phys. J. C* **70** (2010) 51 [[arXiv:1007.2624](#)] [[INSPIRE](#)].
- [53] W. Tung et al., *Heavy quark mass effects in deep inelastic scattering and global QCD analysis*, *JHEP* **02** (2007) 053 [[hep-ph/0611254](#)] [[INSPIRE](#)].
- [54] J. Pumplin et al., *New generation of parton distributions with uncertainties from global QCD analysis*, *JHEP* **07** (2002) 012 [[hep-ph/0201195](#)] [[INSPIRE](#)].